

## Dynamics of an anharmonic oscillator that is harmonically coupled to a many-body system and the notion of an appropriate heat bath

Donald P. Visco, Jr.<sup>1</sup> and Surajit Sen<sup>2,\*</sup>

<sup>1</sup>*Department of Chemical Engineering, State University of New York at Buffalo, Buffalo, New York 14260*

<sup>2</sup>*Department of Physics, State University of New York at Buffalo, Buffalo, New York 14260*

(Received 18 June 1997; revised manuscript received 16 September 1997)

We report extensive numerical studies of the dynamics of a classical particle in an anharmonic one-dimensional potential while it is harmonically coupled to *three* different many-particle systems. The studies address the comparatively simpler dynamical problem when the energy of the anharmonic oscillator is sufficiently low. The *first model* is one in which the many-particle system is a chain of harmonic oscillators that have nearest-neighbor harmonic interactions. The anharmonic oscillator is connected to every harmonic oscillator via harmonic springs. The *second model* is identical to the first except that each oscillator is subjected to an additional one-body harmonic potential. The *third model* is identical to the second except that the nearest-neighbor couplings between the individual harmonic oscillators are absent, i.e., the oscillators are decoupled with respect to one another. In the first model we find that the lowest frequency of the anharmonic oscillator, while possessing a lower bound, increases as  $\omega \propto \sqrt{NK}$ , where  $N$  is the number of oscillators in the bath and  $K$  is the force constant describing the strength of interaction between the anharmonic oscillator and the interacting harmonic many-body system. In the second model we find aspects of dynamical correlations as seen in the canonical ensemble and a dominant frequency that increases as  $\sqrt{NK}$ . We recover the dynamical correlations of the anharmonic oscillator as obtained within the framework of a canonical ensemble [S. Sen, R. S. Sinkovits, and S. Chakravarti, Phys. Rev. Lett. **77**, 4855 (1996)] in the third model for sufficiently many harmonic oscillators. We comment briefly on an alternate way to correctly model heat baths for numerical studies on the dynamics of physical systems using canonical ensembles. [S1063-651X(98)04001-X]

PACS number(s): 05.20.Gg, 05.40.+j

### I. INTRODUCTION

Since most microscopic physical systems are not isolated, the notion of a heat bath to which a physical system is somehow coupled is a convenient construct that enables one to introduce the concept of temperature and make a connection with the laws of thermodynamics and apply them to the system of interest [1]. The canonical ensemble was first postulated by Gibbs and is realized when a system is “weakly coupled” to a heat bath [2] or in the presence of “stray interactions” between the system and the heat bath [3]. An important point to note is that the canonical distribution is independent of the size of the system under study and is therefore valid for even a physical system that consists of a single particle [1]. One can hence regard a canonical ensemble description of a physical system as an idealization that recovers correct thermodynamical response of the system. The question that one can subsequently raise is as follows. Under what circumstances does a system that is somehow coupled to a larger physical system actually exhibit the system dynamics predicted by a canonical ensemble description? The present work concerns a study of this question for a simple, nontrivial physical system, namely, a Duffing oscillator [4].

The dynamics of a single harmonic oscillator in contact with a many-particle system of individual harmonic oscillators, i.e., effectively a heat bath, was probed by van Kampen

[5] and later by Ullersma [6] and Ford, Lewis and O’Connell [7]. Significant literature exists on this problem. It is well understood that one does recover the canonical ensemble dynamics of the harmonic-oscillator system in contact with a heat bath by doing direct analytical calculations in which the detailed dynamics of the heat bath (composed of individual harmonic oscillators that are coupled to the harmonic oscillator that constitutes the system) itself is incorporated into the analysis. In addition, the dynamics of a single massive harmonic oscillator that is connected via harmonic springs with harmonic-oscillator chains to the left and to the right has also been probed in great detail by several workers [8]. It has been shown over a significant intermediate time regime that the relaxation of the heavy mass decays exponentially and that the asymptotic relaxation is oscillatory algebraic and hence the dynamics is different from that of a purely Brownian particle. What is not so clear, however, are the circumstances under which an anharmonic oscillator system, in contact with a large reservoir system that forms the heat bath, adequately describes the canonical ensemble dynamics of the anharmonic oscillator [9]. This is precisely the problem we consider in this article.

To model a heat bath one would need to explicitly state three characteristics of the bath: (i) the type of bath particles, (ii) the interactions between the system and the bath, and (iii) the interactions within the bath itself. The successful model would reproduce known results for relaxation of the anharmonic oscillator in a canonical ensemble [4].

We choose an anharmonic oscillator in a potential with quartic anharmonicity as the system for this study. It is one of the simplest ergodic systems that one can consider for

\*Author to whom correspondence should be addressed.

probing the issues of interest to us. It is simple in the sense that the equation of motion can be solved exactly [10] and ergodic in the sense that the dynamical correlations such as the velocity autocorrelation function of the anharmonic oscillator calculated within the framework of a canonical ensemble show slow relaxation as time goes to infinity, as shown recently in Ref. [4]. A simple interpretation of relaxation for a single anharmonic oscillator in a canonical ensemble is that the oscillator loses the memory of its initial conditions as a function of time.

In the sections to follow we will describe the known canonical ensemble results for the anharmonic oscillator in thermal contact with a heat bath in terms of the dominant frequency associated with its velocity power spectrum at low temperatures. We will then choose three models for the ‘‘internal structure’’ of the heat bath and describe these models in terms of the Hamiltonian of the anharmonic oscillator, the bath, and the coupling between the two. We will give detailed information on the numerical methods used in the study. For each model of the bath, we will show the resulting velocity power spectrum of the anharmonic oscillator when it is harmonically coupled to the bath degrees of freedom. Finally, we will draw conclusions from the work and establish the conditions under which a heat bath can be modeled via a large system with many degrees of freedom.

## II. DYNAMICS IN CANONICAL ENSEMBLES

The Hamiltonian for the anharmonic oscillator is given by

$$E = p^2/2m + (1/2)x^2 + (1/4)x^4, \quad (1)$$

where  $p$  and  $x$  represent the momentum and position coordinates, respectively, of the anharmonic oscillator and  $m$  is the mass of the particle (we set  $m = 1$  for our analysis here). We briefly sketch below the asymptotic analysis that shows that any dynamical correlation function, such as the velocity autocorrelation function, calculated in a canonical ensemble, decays algebraically in time.

The asymptotic analysis was accomplished as follows. We outline below the key steps in the calculations for the Hamiltonian in Eq. (1). The formal solution to the equation of motion is given by [10]

$$x(t) = C \sum_{p=0}^{\infty} a_p \sin(2p+1)\omega t, \quad (2)$$

where the leading terms of the constants  $Ca_n$  are

$$Ca_0 = a,$$

$$Ca_1 = (-a^3/32)(1 - 21a^2/32 + \dots), \dots, \quad (3)$$

and the frequency

$$\omega = (1 + 3a^2/4 + 3a^4/128 + \dots)^{1/2}. \quad (4)$$

In the above expressions, the variable  $a$  is obtained as a function of  $E$  by substituting the formal solutions for  $x(t)$  and  $v(t)$  into Eq. (1), yielding

$$a = (2E)^{1/2} - \frac{9E^{3/2}}{2^{7/2}} \dots. \quad (5)$$

One may observe that the terms on the right-hand side of Eqs. (3)–(5) depend upon the details of the leading anharmonic term in Eq. (1). Therefore, Eqs. (3)–(5) would change if one is to consider a sextic oscillator instead of a quartic oscillator in Eq. (1). The arguments in the analysis presented below, however, would remain invariant for any leading anharmonicity in Eq. (1) [4].

A normalized microcanonical ensemble velocity relaxation function is exactly obtained by substituting  $v(t)$  obtained from Eq. (2) into the equation for the velocity relaxation function

$$\frac{\int_{-\infty}^{\infty} v(t')v(t'+t)dt'}{\int_{-\infty}^{\infty} v(t')^2 dt'} = \frac{\sum_{p=0}^{\infty} a_p^2 (2p+1)^2 \cos(2p+1)\omega t}{\sum_{p=0}^{\infty} a_p^2 (2p+1)^2}. \quad (6)$$

It is difficult to carry out a closed-form energy integral with the result of Eq. (6) to obtain the canonical ensemble velocity relaxation function. We therefore focus on the nature of its asymptotic behavior and start by expanding  $\omega$  in powers of  $\gamma E$ , where  $\gamma$  is a system-dependent constant and is  $3/4$  for the Hamiltonian in Eq. (1). To leading order in  $E$ , we obtain  $\omega \approx 1 + \gamma E$ . For the moment let us ignore the terms with  $p > 0$  and retain only the  $p = 0$  term in the summation of Eq. (6). As we shall show later, the  $p = 0$  term contributes to the slowest decay. Successively faster decays are contributed by the terms with increasing magnitude of  $p$ . We substitute Eq. (6) with the  $p = 0$  term into the expression for the canonical ensemble relaxation function. This gives

$$\frac{\int_0^{\infty} e^{-\beta E} \cos(1 + \gamma E)t dE}{\int_0^{\infty} e^{-\beta E} dE} = \frac{\beta^2 \cos(t) - \gamma \beta t \sin(t)}{\gamma^2 t^2 + \beta^2}, \quad (7)$$

which decays as  $-(\beta/\gamma)\sin(t)/t$  for  $\gamma t \gg \beta$ . It may be noted that we have assumed that the ratio of the density of states to the partition function is essentially constant at low enough energies and hence can be disregarded in the calculation in Eq. (7) [11]. The result on the right-hand side of Eq. (7) is the behavior obtained from the numerical analysis reported in Ref. [4]. The asymptotic functional form is that of  $j_0(t)$ , i.e., the zeroth-order spherical Bessel function. The Fourier transform of the velocity relaxation function exhibits a sharp peak at  $\omega = 1$  for the system described by Eq. (1).

Numerical calculations show that the result in Eq. (7), although originally derived to describe the asymptotic behavior of the velocity relaxation function in the low-temperature limit, applies at all temperatures. This can be shown easily by retaining higher-order terms in  $E$  in the expression for the relaxation function at a fixed energy before substituting into the equation for the canonical relaxation function. Keeping terms  $p > 0$  in Eq. (6) leads directly to the appearance of powers of  $E$  in the integrals, while retaining higher-order terms in the expansion for  $\omega$  leads to trigonometric functions with arguments involving higher powers of  $E$ . This results in contributions to the canonical relaxation function from

integrals of the form  $\int_0^\infty E^p e^{-\beta E} [\cos, \sin](\gamma t E) [\cos, \sin] \times (c_2 t E^2) \cdots dE$ , where the terms in square brackets indicate that one or the other trigonometric function is chosen. Replacing the sin and cos functions containing arguments with powers of  $E$  greater than one with their series expansions simply result in contributions from a sum of integrals of the form  $\int_0^\infty t^l E^m e^{-\beta E} [\cos, \sin](\gamma t E) dE$ , where all of the powers of  $E$  have been collected in  $E^m$ , with  $l$  and  $m$  related by the inequality  $m \geq l + 1$ . In the long-time limit, these integrals have the behavior that they tend to either  $t^{l-m-1}$  or 0, depending on the choice of trigonometric function in the integrand and whether  $m$  is even or odd. Since  $m - l \geq 1$ , all contributions to the velocity relaxation function arising from retaining higher-order terms in  $E$  die off faster than  $1/t$ . In view of the formal similarities between this and the double-well problems, similar results can be derived for the double well [10,11]. It may be noted that the Fourier transform of the velocity power spectrum is sensitive to temperature [4,12].

To summarize this section, we have shown that in canonical ensembles the velocity relaxation function (or any other relaxation functions such as the position or acceleration relaxation functions) decays as  $1/t$  for the quartic anharmonic oscillator [13]. If one performs a Fourier transform of the relaxation functions, one finds a sharp peak in the velocity power spectrum at  $\omega = 1$ . This peak is the dominant one at low temperatures, as shown in Ref. [4]. Although it remains at all temperatures, higher-frequency effects tend to mask its presence at high enough temperatures.

We now proceed to make specific models for the heat bath itself and study the velocity power spectrum of the anharmonic oscillator in Eq. (1) when it is coupled to the various models for the bath. For the sake of simplicity, we shall focus on the low-energy dynamics of the anharmonic oscillator for the various circumstances that we shall consider below.

### III. HEAT BATH MODELS

#### A. Model 1

The Hamiltonian for the anharmonic oscillator that is harmonically coupled to the bath described by a harmonic-oscillator chain model is given by

$$H = p^2/2m + (1/2)x^2 + (1/4)x^4 + \sum_{i=1}^N p_i^2/2m_i + \sum_{i=1}^{N-1} \frac{K_i}{2} (x_i - x_{i+1} + l)^2 + \frac{K}{2} \sum_{i=1}^N (x - x_i + il)^2. \quad (8)$$

In Eq. (8), every particle in the harmonic-oscillator chain is coupled by springs with spring constant  $K_i$  and the anharmonic oscillator is also coupled with each of the oscillators in the chain with the spring constant  $K$ . We regard  $l$  as the equilibrium distance between the particles that reside on the harmonic-oscillator chain. We have probed the dynamics of the anharmonic oscillator in this model for various choices of  $K_i$  and  $K$ . Our calculations show that our conclusions are robust against the choices of  $K_i$  we had explored. The details are discussed in Sec. IV below.

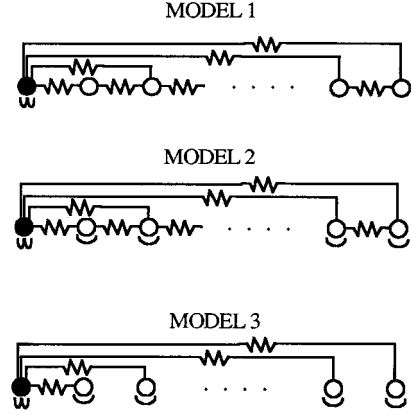


FIG. 1. Cartoons describing the interactions in the three models. The filled circle is the particle in the anharmonic well. The open circles are the bath particles. The parabola under some bath particles indicate that those particles are in a harmonic well. The resistors are harmonic springs.

#### B. Model 2

The Hamiltonian for the anharmonic oscillator that is harmonically coupled to the bath described by the harmonic-oscillator chain with each oscillator in a harmonic potential well is given by

$$H = p^2/2m + (1/2)x^2 + (1/4)x^4 + \sum_{i=1}^N p_i^2/2m_i + \sum_{i=1}^N (1/2)x_i^2 + \frac{K}{2} \sum_{i=1}^N (x - x_i + il)^2 + \sum_{i=1}^{N-1} \frac{K_i}{2} (x_i - x_{i+1} + l)^2. \quad (9)$$

To reiterate, model 2 is exactly model 1 except the bath particles of model 2 are in a harmonic potential well. As we shall see, in spite of the obvious similarities between models 1 and 2, their dynamics are distinct. Therefore, the studies of models 1 and 2 prompted us to consider model 3, described below.

#### C. Model 3

The Hamiltonian for the anharmonic oscillator that is harmonically coupled to the bath described by the free harmonic oscillators is given by

$$H = p^2/2m + (1/2)x^2 + (1/4)x^4 + \sum_{i=1}^N p_i^2/2m_i + \sum_{i=1}^N (1/2)x_i^2 + \frac{K}{2} \sum_{i=1}^N (x - x_i + il)^2, \quad (10)$$

Once again, model 3 is exactly model 2 except the bath particles of model 3 are now uncorrelated. In the three models described by Eqs. (8)–(10)  $m = m_i = 1$  and  $x_i$  and  $p_i$  are the position and momentum of the bath particles, respectively, and  $N$  is the total number of oscillators in the bath. Cartoon descriptions of the interactions in all three models are show in Fig. 1.

#### IV. NUMERICAL STUDY

It is very difficult to solve for the dynamical behavior of the anharmonic oscillator in models 1–3 in an analytic fashion. The equations of motion for each of the particles in models 1–3 were therefore solved numerically using the velocity version of the Verlet algorithm [14]. The anharmonic oscillator was assigned an initial velocity of  $v=0.001$  and an initial position of  $x=0$ . This initial condition sets the anharmonic oscillator and the bath particles in motion. The particles used to construct the baths in models 1 and 2 were all initially at rest and initially located on the number line according to  $x_i=0.0001i$ , where the index ran from  $i=1,\dots,N$  where  $N$  was the number of harmonic oscillators used in the study. Thus  $l=0.0001$ . The  $K_i$ 's were varied randomly in the interval  $[0.01,1.0]$ . We have also studied cases in which  $K_i=K$ . Our calculations reveal that varying  $K_i$  has no significant effect on the frequency spectrum of the anharmonic oscillator in the interval explored above. Therefore, we have set all the  $K_i$ 's equal to  $K$  in all the work reported here for models 1 and 2. The insensitivity of the results to the values of  $K_i$  chosen is possibly due to the fact that the velocities of the particles in the harmonic-oscillator chains are rather small. However, as we shall see, the dynamics of the anharmonic oscillator is sensitive to any one-body potential that the bath particles are subjected to as well as the details of the two-body interactions within the bath. Thus the frequency spectrum of the anharmonic oscillator in model 2, in which the bath particles in the harmonic-oscillator chain are subject to a one-body potential, is distinct from that in model 1, in which the bath particles in the harmonic-oscillator chain have no additional constraints. Likewise, the frequency spectrum of the anharmonic oscillator in model 2, which has nearest-neighbor interactions of the bath particles, is different from that obtained using model 3, which has no interactions between the bath particles.

In the study of model 3, the velocities of the harmonic oscillators that were used to construct the bath were distributed such that the initial kinetic energy of these oscillators were Boltzmann weighted according to  $\exp(-\kappa E_K)$ , where  $E_K$  is the initial kinetic energy and  $\kappa$  is some constant (we set  $\kappa=1$ ). The range of kinetic energies allowed was  $10^{-4}$ –25.32. Thus we had equal spacing in  $\exp(-\kappa E_K)$ , but unequal (i.e., Boltzmann weighted) kinetic-energy spacing. The initial positions of the harmonic oscillators in this model were chosen as per models 1 and 2.

The integration step size and the time length of the study varied depending on the set of  $N$  and  $K$  being studied. The largest step size used was  $10^{-2}$  time units, while the smallest was  $10^{-4}$  time units. The length of time over which the velocity relaxation functions of the anharmonic oscillator were determined averaged to near 50 time units.

We have used the discrete cosine transform [15] of the velocity relaxation function to determine the velocity power spectrum of the anharmonic oscillator. In order to eliminate the negative numbers that arise from incomplete phase cancellations in the calculation of the discrete cosine transform, we have multiplied the relaxation function with a Gaussian function of the form  $\exp(-\alpha t^2)$  before taking the transformation. All the velocity power spectra shown in this study have used this Gaussian function with  $\alpha=0.02$ .

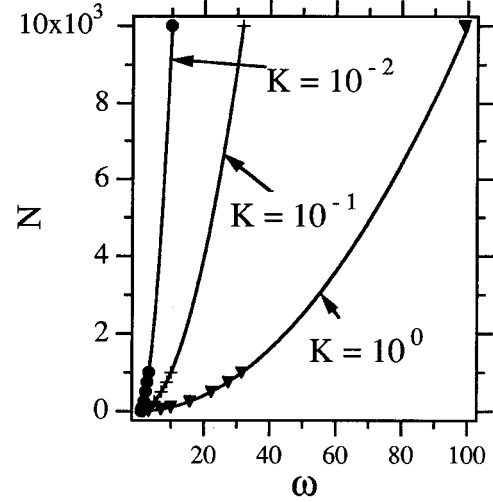


FIG. 2. Dominant frequency  $\omega$  of the velocity power spectrum for the anharmonic oscillator connected to the bath as described by model 1. The symbols correspond to the simulations done at various sets of  $(N, K)$ , where  $N$  is the number of bath particles and  $K$  is the spring constant for all the springs. The parabolas have the form  $N(\omega, K) = -1 - 1/K + (1/10)K^{-0.693}\omega + (1/K)\omega^2$ .

#### V. DYNAMICS IN MODEL SYSTEMS

In this section we shall discuss our studies on the velocity relaxation function for the anharmonic oscillator that is harmonically coupled to the various heat baths (described by models 1–3) under study. For model 1, i.e., the bath modeled using the harmonic-oscillator chain, we have studied the 30 velocity power spectra that can be obtained from the following sets of  $(N, K) = (N=1, 2, 9, 49, 99, 249, 499, 749, 999, 9999; K=0.01, 0.1, 1)$ . Recall that we have set each  $K_i$  equal to  $K$  in models 1 and 2. We have found no evidence of a peak in the velocity power spectrum at  $\omega=1$ . [Recall the discussion following Eq. (6).] This leads us to conclude that the dynamics of the bath particles strongly affects the dynamics of the anharmonic oscillator to which the bath particles are coupled via  $K$ . We did, however, find peaks in the velocity power spectrum of the anharmonic oscillator at values of  $\omega$  that were greater than 1. These results are summarized in Fig. 2.

A subsequent analysis of the quadratic fits of  $N$  as a function of  $\omega$ , the lowest frequency of the anharmonic oscillator, for the three values of  $K$  characterizing the coupling between the anharmonic oscillator and the particles in the harmonic-oscillator chain studied resulted in an empirical expression for  $N$  as a function of  $N$  and  $K$ , which is given by

$$\omega = - (1/20)K^{1-0.693} + (1/20)\sqrt{K^{2(1-0.693)} + 400NK + 400K + 400}. \quad (11)$$

It may be that one can write Eq. (11) as

$$\omega = - (1/20)K^{1-\ln 2} + (1/20)\sqrt{K^{2(1-\ln 2)} + 400NK + 400K + 400}. \quad (12)$$

However, in the absence of an analytical proof, it is worth not speculating that a fitted parameter such as 0.693 is actually  $\ln 2$ .

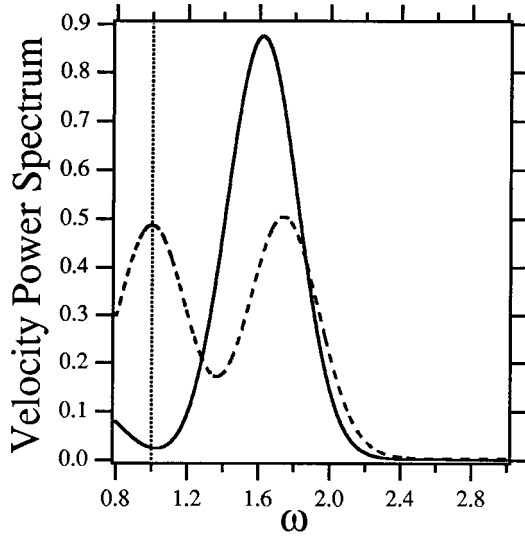


FIG. 3. Velocity power spectrum for the anharmonic oscillator connected to the bath as described by model 1 (solid line) and model 2 (dashed line) for  $N=1$ ,  $K=1$ . The vertical line at  $\omega=1$  is to indicate the canonical ensemble frequency.

For large  $N$ , this becomes

$$\omega \propto \sqrt{NK}. \quad (13)$$

Let us recall that the anharmonic oscillator couples with each harmonic oscillator via springs of spring constant  $K$  and that  $N$  is the total number of harmonic oscillators that interact with the anharmonic oscillator. It then becomes apparent that one can regard the collective effect of the oscillators on the dynamics of the anharmonic oscillator as that of a single one that oscillates with a harmonic coupling of  $NK$ . This “effective megaoscillator” adds a “harmonic frequency” to the velocity power spectrum of the anharmonic oscillator.

The role of the harmonic interactions between the particles that make up the bath is not evident from the analyses of model 1. As we shall see below, the harmonic coupling between the particles tends to suppress the dynamical effects of the anharmonic oscillator.

When we model the bath according to model 2 [see Eq. (9)], we find that for the state where  $N=1$ ,  $K=1$ , we observe two frequencies: the first at  $\omega=1$  and the second at a frequency that is consistent with the  $\omega$  value suggested by Eq. (11). The velocity power spectra of the anharmonic oscillator in this bath (i.e., in model 2) as well as that in model 1 with  $N=1$  and  $K=1$  are shown in Fig. 3. It would seem that the bath described by model 2 does lead to the correct canonical ensemble frequency. While this is encouraging, we also note that the bath in model 2 leads to other peaks (as shown in Figs. 3 and 4). The peak at  $\omega=1$  turns out to become increasingly less dominant as  $N$  is increased in model 2. Thus, for  $N=999$ ,  $K=1$ , we find that the peak at  $\omega=1$  is dominated by a high-frequency peak at a location that is consistent with expectations based upon the proportionality given in Eq. (13). This is shown in Fig. 4. The inset of Fig. 4 shows that there is still a peak at  $\omega=1$ , but it possesses an amplitude that is  $\sim 1/N$  if we assume that the peak at  $\omega=31.6$  is of amplitude unity. The results in Figs. 3 and 4 confirm the role

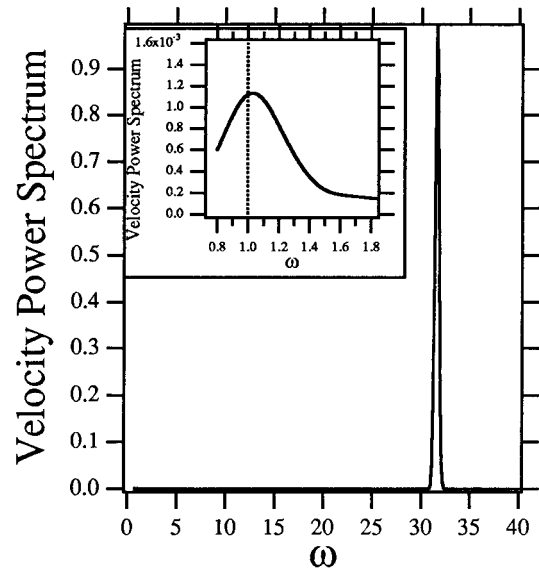


FIG. 4. Velocity power spectrum for the anharmonic oscillator connected to the bath as described by model 2 for  $N=999$ ,  $K=1$ . The inset shows the existence of a peak near  $\omega=1$  that cannot be seen when plotted with the dominant frequency. The vertical line at  $\omega=1$  is to indicate the canonical ensemble frequency.

of the size of the bath in this problem, namely, that for large  $N$ , the high-frequency contributions are dictated by  $N$  itself. When the bath particles are coupled with one another, the natural frequency of the anharmonic oscillator is dwarfed by the frequencies associated with the size of the bath and the interactions between the bath particles.

If we remove the coupling between the harmonic oscillators in the chain (i.e., make the bath particles uncorrelated and consider a set of free harmonic oscillators as in model 3) and recalculate the velocity power spectrum of the anhar-

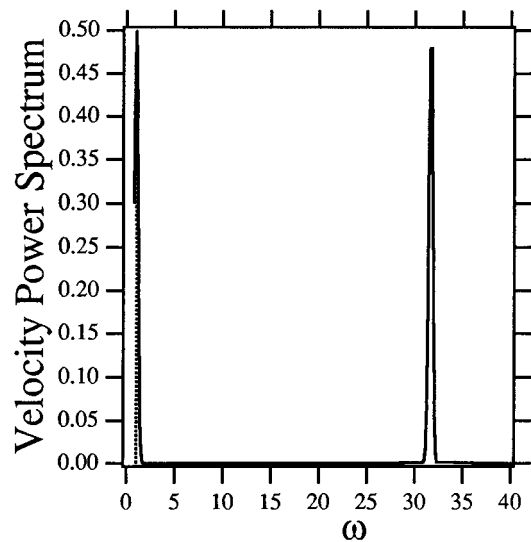


FIG. 5. Velocity power spectrum for the anharmonic oscillator connected to the bath as described by model 3 for  $N=999$ ,  $K=1$ . The vertical line at  $\omega=1$  is to indicate the canonical ensemble frequency.

monic oscillator, we readily recover the canonical ensemble peak at  $\omega = 1$  for the  $N = 999$ ,  $K = 1$  system as shown in Fig. 5. Thus model 3 is clearly a better description of a heat bath than models 2 and 1. However, even this model is not perfect. The peak in the velocity power spectrum at  $\omega = 31.6$  in Fig. 5 still persists and has an amplitude almost equal to that of the peak at  $\omega = 1$ . It appears that the lone important peak from model 2 at this state has split into two equally important peaks when the bath particles are uncoupled (model 3).

As argued above, the peak at  $\omega = 31.6$  from model 3 at  $N = 999$ ,  $K = 1$  is related to the size of the bath. In the thermodynamic limit, this peak will move to infinitely high frequencies and hence will not affect the dynamics of the system being probed. The amplitude of the peak at unity is no longer suppressed by the high-frequency peak in model 3. This is attributed to the fact that the bath particles are not coupled with each other and thus the collective frequencies associated with the dynamics of the bath particles can no longer affect the dynamics of the system itself.

To summarize this section, we have shown that among the models we have probed in this study, model 3 is the most appropriate one for describing a heat bath. For any finite bath

constructed out of harmonic oscillators, there are high-frequency “contaminants” to the dynamics of the system of interest. However, in addition to the above-mentioned contaminant frequencies, if the bath particles are uncoupled from one another, the dynamics of the system of interest is unaffected by the details of the bath. The contaminant frequencies can be readily characterized in a numerical study. For a sufficiently large bath, these high-frequency corrections can be made to lie beyond the highest frequencies allowed by the shortest time scales supported by the system. Thus a model similar to model 3 can be a useful approach to model a heat bath in simulational studies on the dynamics of physical systems in a canonical ensemble [16].

#### ACKNOWLEDGMENTS

D.P.V.J. would like to thank the Department of Chemical Engineering at SUNY Buffalo for the computing time necessary to complete this study. S.S. thanks R. S. Sinkovits, S. Chakravarti, and S. D. Mahanti for their interest in this work. This work has been supported by the Office of the Provost at SUNY Buffalo (S.S.) and by the U.S. Army (S.S.).

- 
- [1] C. J. Thompson, *Classical Equilibrium Statistical Mechanics* (Oxford Science Publications, New York, 1988).
  - [2] J. W. Gibbs, *Elementary Principles in Statistical Mechanics* (Charles Scribner’s Sons, New York, 1902).
  - [3] R. C. Tolman, *The Principles of Statistical Mechanics* (Oxford University Press, London, 1938).
  - [4] S. Sen, R. S. Sinkovits, and S. Chakravarti, *Phys. Rev. Lett.* **77**, 4855 (1996); *Physica A* **225**, 292 (1996).
  - [5] N. G. van Kampen, *K. Dan. Vidensk. Selsk. Mat. Fys. Medd.* **26**, No. 15 (1951).
  - [6] P. Ullersma, *Physica (Amsterdam)* **32**, 27 (1966); **32**, 56 (1966); **32**, 74 (1966); **32**, 90 (1966).
  - [7] G. W. Ford, J. T. Lewis, and R. F. O’Connell, *J. Stat. Phys.* **53**, 439 (1988).
  - [8] See D. Vitali and P. Grigolini, *Phys. Rev. A* **39**, 1486 (1989), and references therein; S. Sen, Z.-X. Cai, and S. D. Mahanti, *Phys. Rev. Lett.* **72**, 3287 (1994).
  - [9] S. D. Mahanti, G. Zhang, and G. Kemeny, *Phys. Rev. B* **35**, 8551 (1987).
  - [10] H. T. Davis, *Introduction to Nonlinear Differential and Integral Equations* (Dover, New York, 1962), p. 291.
  - [11] S. K. Sarkar, *Phys. Rev. E* **54**, 2465 (1996); J. P. Codaccioni and R. Caboz, *J. Math. Phys.* **24**, 2436 (1984).
  - [12] R. S. Sinkovits and S. Sen (unpublished).
  - [13] It has been shown in Refs. [4] and [11] that the  $1/t$  relaxation is generic to *all* one-dimensional potentials that have leading quartic anharmonicity. The examples therefore include the  $\cosh x$  and the Gaussian potentials.
  - [14] M. P. Allen and D. J. Tildesley, *Computer Simulation of Liquids* (Oxford Science Publications, New York, 1987).
  - [15] W. H. Press, S. A. Teukolsky, W. T. Vetterling, and B. P. Flannery, *Numerical Recipes in Fortran*, 2nd ed. (Cambridge University Press, New York, 1992).
  - [16] D. P. Visco, Jr. and S. Sen (unpublished).